

Sounding the metabolic orchestra: A delay dynamical systems perspective on the glucose-insulin regulatory response to on-off glucose infusion

Stefan Ruschel^{1,2,*} and Benoit Huard^{1,+}

¹Northumbria University, Department of Mathematics, Physics and Electrical Engineering, Newcastle upon Tyne, NE1 8ST, United Kingdom

²The University of Auckland, Department of Mathematics, Auckland, 1142, New Zealand

*stefan.ruschel@northumbria.ac.uk

+benoit.huard@northumbria.ac.uk

ABSTRACT

We investigate the consequences of periodic, on-off glucose infusion on the glucose-insulin regulatory system on the basis of a system-level mathematical model with two explicit time delays. Studying the effects of such infusion protocols is mathematically challenging yet a promising direction for probing the system response to infusion. We pay special attention to the interplay of the infusion with intermediate-time-scale, ultradian oscillations that arise as a result of the physiological response of glucose uptake and back-release into the bloodstream. By using numerical solvers and numerical continuation software, we investigate the response of the model to different infusion patterns, and explore how these patterns affect the overall levels of glucose and insulin, and can lead to entrainment. By doing so, we provide a road-map of system responses that can potentially help identify new test strategies for detecting abnormal responses to glucose uptake.

Introduction

Cyclic rhythms are widely recognized for their significant role in regulating the function of biological and physiological systems^{1,2}. Endogenous oscillations are typically encountered in healthy individuals, while a progressive lack of control of these rhythms is often associated with system stress (e.g. sleep deprivation^{3,4}), and disease evolution in humans⁵.

A prominent example of such endocrine oscillations in the human body is the self-regulation of blood glucose levels⁶. When blood glucose levels increase, insulin is released from the pancreas. Insulin then causes blood glucose levels to decrease by stimulating body cells to absorb glucose from the blood. Conversely, when blood glucose levels fall, pancreatic β -cells release glucagon stimulating hepatic glycogenolysis and neoglucogenesis. The level of blood glucose is then controlled by the rates of insulin secretion (activation by glucose) and hepatic glucose production (inhibition by insulin). Within the glucose-insulin regulatory system, both rapid oscillations of insulin (period \sim 6-15 minutes), and ultradian oscillation of glucose and insulin (of similar period \sim 80-180 minutes⁷) have been observed during fasting, meal ingestion, continuous enteral and intravenous nutrition⁸.

The most important pathway to understand the underlying mechanisms of these glucose-insulin oscillations is measuring the response to glucose infusions. A large quantity of metrics and mathematical models have been devised for that purpose. While the HBA1c metric remains an essential tool for the diagnostic, prevention and control for T2 diabetes⁹, clinical tests involving patterns of glucose intake combined with mathematical models provide a mechanism for evaluating the efficacy of internal regulation¹⁰⁻¹³. The minimal model devised by Bergman and Cobelli^{14,15} provides an effective method for estimating insulin sensitivity from an intravenous or oral glucose tolerance test, although it can lead to underestimation in individuals with a large acute insulin response¹⁶. With the wider availability of continuous glucose monitors and automated insulin pumps, the ability to detect diabetic deficiencies relies on the capacity of models to reproduce more complex and realistic dynamics under various routine life conditions such as, for example, sleep deprivation³.

The main goal of this article is to identify the types of behaviors in a suitable mathematical model that can be expected as a response to periodic glucose uptake, specifically periodic on-off glucose infusion, which can be readily implemented in practice. We focus on the capacity of the system to fall into lockstep with the frequency of the glucose stimulus (so-called entrainment) which has been observed in numerous contexts at the ultradian and circadian levels in endocrinology^{13,17,18},

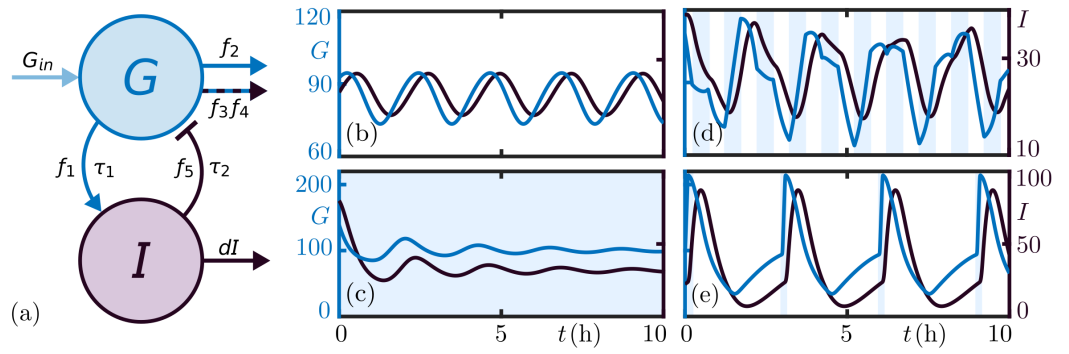


Figure 1. Panel (a): Diagrammatic overview of the glucose-insulin regulatory delayed-feedback model (1)–(2); see methods section for details. Panels (b)–(e): Characteristic time series of system (1)–(2) (with positive initial condition) for different patterns of glucose infusion with intervals of fasting indicated by a white background and intervals of glucose infusion with constant rate indicated by a light blue background. Units are $[G]$ mg dl⁻¹, $[I]$ mg dl⁻¹, and $[t]$ h. Infusion rates when not fasting are $G_{\text{in}} = 1.35$ mg dl⁻¹ min⁻¹ in panels (c)–(d) and $G_{\text{in}} = 24.3$ mg dl⁻¹ min⁻¹ in panel (e); period of infusion is $T_{\text{in}} = 1$ h in panel (d) and $T_{\text{in}} = 3$ h in panel (e); time of infusion is $t_{\text{in}} = 30$ min in panel (d) and $t_{\text{in}} = 5$ min in panel (e).

but especially in models of glucose-insulin oscillations with periodic infusion¹⁹.

Many modeling efforts have been made to replicate the nonlinear response of the glycolytic system; in particular, the mathematical modeling of the delayed response of individual parts of the system by explicit time delays has proven an effective means to explain the onset of self-sustained, ultradian oscillations in the glycemic system^{20–22}. A common approach to modeling oscillatory behavior of complex biology is to consider time delays²³. In particular, models of endocrine regulation often incorporate explicit delays to account for the time required for the synthesis, release, and action of hormones or metabolites¹⁷. Various models of intrapancreatic rhythmic activity have been proposed recently, see Ref. 13 for a review. For example, it was shown that glucose oscillations can enhance the insulin secretory response at the β -cell level when tweaked at a suitable amplitude and frequency²⁴. Negative delayed feedback has also been shown to provide a suitable explanatory mechanism for the coordinated pancreatic islet activity²⁵.

In this article, we investigate a two-component, system-level mathematical model (see Eqs. (1)–(2) in the methods section) for blood glucose level $G(t)$ and insulin levels $I(t)$ with two explicit time delays τ_I and τ_G corresponding to pancreatic insulin and hepatic glucose production pathways, see the methods section for details on the model. The model incorporates the following physiological processes and factors that influence glucose and insulin dynamics, see Fig. 1(a) for a schematic overview.

- Glucose uptake: G_{in} represents glucose uptake into the blood by meal ingestion, continuous enteral or intravenous nutrition.
- Insulin production: f_1 represents the production of insulin. It is influenced by the concentration of glucose with a delay τ_I to account for the time lag between high glucose levels triggering insulin production in the pancreas and when it becomes available for reducing glucose in the bloodstream.
- Insulin-independent glucose utilization: f_2 describes the utilization of glucose by tissues, mainly the brain, in an insulin-independent manner. It does not rely on the presence of insulin.
- Insulin-dependent glucose utilization: $f_3 \cdot f_4$ represents the utilization of glucose by muscle tissues in an insulin-dependent manner. It reflects the capacity of tissues to utilize insulin for glucose uptake.
- Glucose production by the liver: f_5 represents the production of glucose by the liver. The delay τ_G represents the time between hepatic glucose production and insulin stimulation.
- Insulin degradation: The rate d accounts for the degradation of insulin in the body, primarily by the liver and kidneys. It combines both natural factors (e.g., exercise) and artificial factors (e.g., medication) that influence the rate of insulin degradation.

The nonlinear pathways f_1, f_2, f_3, f_4 , and f_5 are represented using Hill functions, which are mathematical functions commonly used in biological modeling. These functions introduce additional parameters that have specific physiological interpretations and allow for a more accurate represen-

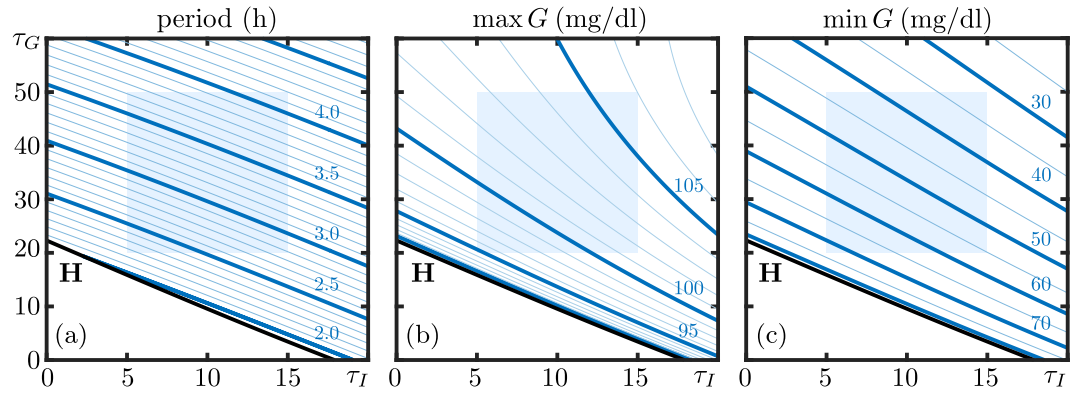


Figure 2. Characterization of fasting oscillations with respect to response delays. Panels show the period (a), maximum glucose value (b), and minimum glucose value (c) as a function of response delays τ_I (min) and τ_G (min). Shown are the critical curve for oscillations (black, Hopf bifurcation), and iso-curves (blue) with constant period (a), glucose-maxima (b) and minimum of G (c). The light blue rectangle shows the physiological range of delay values for comparison. See methods section for the model and choice of parameters.

tation of the underlying dynamics of the glucose-insulin system, see methods section for details. The delays τ_I and τ_G are important physiological parameters encapsulating the responsiveness of the signaling and production pathways. They are assumed to be constant for the purpose of this article, although in practice, they can vary between individuals, as well as during the day and lifespan, and especially in the presence of diabetes.

The model has been extensively analyzed by various authors in the case of constant rates of glucose infusion^{20,26–28}. It originates from the work of Sturis and collaborators who devised a model of glucose and insulin ultradian oscillations which were observed experimentally under various conditions²⁹. We also remark here that the model belongs to a larger class of models incorporating delays to capture secretion processes^{11,30}. We extend these earlier efforts on the analysis of the model by studying its response to periodic variations of the parameter G_{in} , that is, periodic variations of glucose uptake. In particular, we consider on-off infusion, a form of periodic infusion that is comparatively easy to implement in practice, where the rate of glucose infusion periodically switches between a positive constant value and zero. Panels (b)–(e) of Fig. 1 show prototypical examples for the response of system (1)–(2) for various types of glucose uptake during fasting (b), glucose infusion with a (relatively high) constant rate (c) and periodic on-off infusion (d)–(e). We first investigate the loss of ultradian oscillations under sufficiently strong constant infusion, see Fig. 1(b)–(c). We then aim to study the effects of different glucose infusion patterns G_{in} on glucose homeostasis, in particular the transition from quasi-periodicity to entrainment, as shown in Figs. 1(d)–(e).

Results

Ultradian oscillations

It has been shown that for a fixed constant glucose infusion G_{in} , sufficiently large values of the response delays τ_1 and τ_2 lead to periodic oscillations in system (1)–(2) with periods closely resembling the observed range for ultradian oscillations^{20,27,28}. Mathematically speaking, the onset of oscillations is mediated by a supercritical Hopf bifurcation that leads to a local topological change in the solution space of system (1)–(2) from a stable equilibrium to a situation of an unstable equilibrium surrounded by a small stable limit cycle close to the bifurcation point²⁶. For details on bifurcation theory and the Hopf bifurcation, we refer the interested reader to Ref. 31. To witness the bifurcation point, it is necessary to vary at least one parameter of the system. Here, we focus on the response delays τ_I and τ_G . Allowing these two parameter values to vary simultaneously, one obtains a one-parameter curve $\mathbf{H}(\omega) = (\tau_I(\omega), \tau_G(\omega))$ of Hopf bifurcation in the (τ_I, τ_G) -plane in terms of the Hopf frequencies ω , see Methods section for a detailed derivation. The curve $\mathbf{H}(\omega)$ corresponds to the critical curve for oscillations in system (1)–(2).

Figure 2(a) shows the curve \mathbf{H} (black) during fasting, i.e. for $G_{in} = 0$, computed with the software package DDE-Biftool for Matlab^{32,33}. It has been numerically verified that the curve \mathbf{H} is indeed supercritical for the range of parameter values considered. Figure 2(a) can be interpreted as follows: First, for value pairs above the curve and for $\tau_I \leq 20$ min, $\tau_G \leq 60$ min, any solution of the model starting in a physiological range of glucose and insulin develops periodic oscillations, see Fig. 1(b). Second, for value pairs (τ_I, τ_G) below the curve \mathbf{H} , oscillations in system (1)–(2) decay and approach

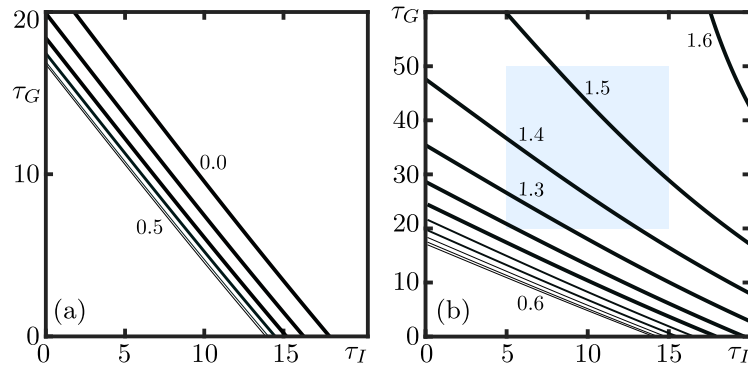


Figure 3. Position of the critical curve (curve of Hopf bifurcation) in the (τ_I, τ_G) -plane for various values of G_{in} ranging from 0 to 0.5 and from 0.6 to 1.6 $\text{mg dl}^{-1} \text{min}^{-1}$ (all black). The light blue rectangle shows the physiological range of delay values for comparison.

the equilibrium (G^*, I^*) . This possibly reflects the situation where an individual is administered a glucose dose that is too high to be managed in an oscillatory manner within physiological glucose and insulin ranges, compare Fig. 1(c).

Figure 2(a) also gives an overview of the resulting period of oscillation above the critical curve **H** shown in the form of isocurves (blue) of limit cycles with constant period. The physiological range of parameters (τ_I, τ_G) is highlighted by light blue square in the background for convenience. The range of expected periods for ultradian oscillations as predicted by the model thus ranges from 2.2 to 4.2 hours during fasting. More generally, we observe the period of the limit cycle oscillation grow approximately linear with the sum of the two delay values $\tau_I + \tau_G$. We also observe that away from the curve **H**, the limit cycle oscillation becomes less and less sinusoidal, i.e. the nonlinearity of system (1)–(2) has more and more of an effect on the limit cycle. Panels (b)–(c) of Fig. 2 illustrate this effect by plotting isocurves of periodic orbit with constant minimum and maximum glucose within one period of oscillation. We observe that, whereas the glucose minimum decreases approximately linearly with the sum of the delays $\tau_I + \tau_G$, the maximum G remains almost constant for the range of parameter values considered. Note that this predicted effect of long response delays is potentially harmful and is virtually undetectable by common testing methods.

On the other hand, we observe that, for fixed values of the delays, gradually increasing the glucose infusion leads to a loss of oscillations. This phenomenon has been observed before and can be interpreted as an insufficient insulin secretion to accommodate the infusion, forcing the system to lower glucose lower levels²⁶. Figure 3 shows how the location of the curve **H** changes for various levels of constant glucose infusion. We observe a two different types of change for values in the approximate ranges $0 \leq G_{in} \leq 0.55 \text{ mg dl}^{-1} \text{min}^{-1}$ and $G_{in} > 0.55 \text{ mg dl}^{-1} \text{min}^{-1}$ shown in panels (a) and (b) of Fig. 3, respectively. Figure 3(a) suggests that low levels of G_{in} promote oscillations in system (1)–(2) as compared to the fasting case. This trend reverses at approximately at $G_{in} = 0.55 \text{ mg dl}^{-1} \text{min}^{-1}$, where the location of the curve **H** starts moving to larger and larger values of τ_I and τ_G , see Fig. 3(b). Approximately at $G_{in} = 1.2 \text{ mg dl}^{-1} \text{min}^{-1}$ the position of **H** is comparable with the starting location for $G_{in} = 0$. Further increasing G_{in} moves **H** inside the physiological range of delay values (light blue) and finally beyond causing all oscillations to cease in the physiological parameter regime. Compare also Fig. 1(b)–(c) for an illustration of this transition and the loss of oscillations for $(\tau_I, \tau_G) = (5, 20)$.

Entrainment and amplitude response to on-off glucose infusion

We now investigate the effect of periodic glucose infusion on baseline fasting oscillations shown in Fig. 1(b), i.e. we fix $\tau_I = 5 \text{ min}$, $\tau_G = 20 \text{ min}$ and periodically adjust the level of G_{in} between 0 and a positive value G_0 to be specified. The natural frequency of ultradian oscillation in this case is $T \approx 2.2 \text{ h}$. We show that the resulting glucose and insulin ranges depend sensitively on the period of the on-off infusion. Figures 1(d)–(e) show two of the possible outcomes with different maximal infusion strength G_{max} , period of infusion T_{in} , and infusion duration t_{in} .

Long infusion time compared to period Figure 1(d) shows the result of periodic infusion with $G_{in} = 1.35 \text{ mg dl}^{-1} \text{min}^{-1}$, for $t_{in} = 30 \text{ min}$ every $T_{in} = 60 \text{ min}$, resulting in so-called quasi-periodic oscillations. Indeed, quasi-periodic oscillations are characterized by the presence of an oscillating envelope of the oscillation that evolves on a much slower time-scale, compare Fig. 1(d). This is in sharp contrast with panels (b) (no infusion) and (c) (constant infusion with the same maximum rate) of Fig. 1, where we have either periodic oscillations, or a decay of oscillations towards the

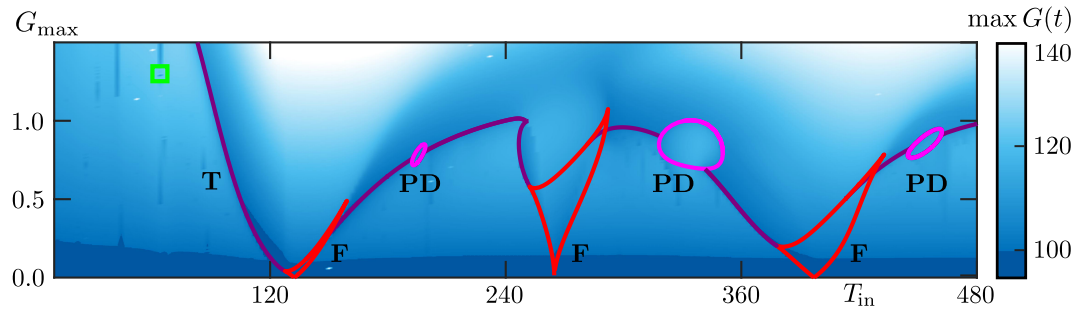


Figure 4. Response of model (1)–(2) to glucose infusion protocol (13) with maximum infusion rate G_{\max} (mg/(dl min)) and length of infusion $t_{\text{in}} = T_{\text{in}}/2$ (h). Shown is the maximum value of G (mg/dl) in colorcode (blue-white) obtained by integration for various T_{in} and G_{\max} over $100(\tau_I + \tau_G + T_{\text{in}})$ time units. The maximum data is overlaid by curves of torus bifurcation (purple), curves of fold bifurcation of periodic orbits (red) and curves of period doubling bifurcation (magenta) bounding regions of locking to the infusion protocol. Other parameters are $\tau_I = 5$ min and $\tau_G = 20$ min.

equilibrium state. Quasi-periodic oscillations can be expected to occur in oscillatory systems which are externally driven by an input with non-commensurable period, here $T_{\text{in}}/T_0 = 2.2$. In this case, the effect of infusion very much depends on its current state: When insulin is low, glucose increases quickly; when insulin is high, glucose cannot increase further and the infusion only delays the expected decrease in glucose levels.

Periodicity of the oscillations can be restored by adjusting G_{in} and T_{in} . Figure 4 summarizes the response of system (1)–(2) to periodic forcing with different values of G_{in} and T_{in} . The locus in parameter space of the quasi-periodic oscillation shown in Fig. 1(d) is indicated by a green rectangle. Figure 4 shows the overall glucose maximum (in color code) observed over a time span of $100 \cdot (T_{\text{in}} + \tau_I + \tau_G)$ minutes. The various mechanisms generating periodic rhythms can be understood from the numerically computed bifurcation curves shown in 4. These correspond to curves of torus bifurcations **T** (purple), curves **F** (red) of fold (or saddle-node) bifurcations of periodic orbits, and curves **PD** (magenta) of period-doubling bifurcations of periodic orbits. These mark the transition to periodic solutions and thus characterize the so-called *entrainment* of oscillations.

The curves **F** respectively enclose deltoid-like regions – called resonance or locking tongues – extending from the line $G_{\text{in}} = 0$, inside of which we observe periodic oscillations. The curves **F** emerge pairwise from resonant points where the infusion period is a rational multiple of the natural period of the system without infusion, i.e. $pT_{\text{in}} = qT_0$ for integers p, q . Figure 4 shows the first three principal resonances of system (1)–(2) where $p = 1, 2, 3$ and $q = 1$. It is expected that such resonance tongues emanate from the line G_{\max} at every rational point T_0 . These higher order resonances (except $p = 4$ and $q = 1$ which is outside of the considered range of parameter values) has been omitted/not computed as they are typically very narrow and thus unlikely to be physiologically relevant.

This behavior persists moving towards larger values of G_{\max} into the regions that are bounded approximately by the curves **T**, where the underlying stable periodic orbit destabilizes and gives rise to a torus that corresponds to quasi-periodic oscillations. We find numerical evidence that the direction with which this torus emanates from the the curve **T** can change and gives rise to the discontinuous transition between the observed maximum values in Fig. 4. The curves **T** each emanate from either point of intersection with a curve **F** or **PD**. Intersections with curves **PD** correspond to higher order locking between the ultradian oscillations and the infusion. Overall, we observe that the strength and period of the infusion have a crucial effect on the resulting amplitude of the oscillations. For instance, forcing the system periodically with $T_0 = T_{\text{in}}$ and relative amplitude $G_{\text{in}} = 1 \text{ mg dl}^{-1} \text{ min}^{-1}$ leads to a 40% increase of the overall amplitude of the oscillation (which appears to be still in physiological range). In contrast, stimulating the system with a gradually increasing G_{in} in the 2:1 regime first goes through phase during which glucose amplitudes remain relatively constant before slowly increasing.

More generally, we observe that, for the assumed values of the response delays, periodic infusion with $T_{\text{in}} = 2t_{\text{in}} > T_0$ and G_{in} is sufficient for the resulting period of the resulting glucose-insulin oscillation to be set by (locked to) the period of glucose infusion.

Short infusion time compared to period We note here that locking can be achieved when the same glucose dose is delivered in a shorter period of time, resulting in a more concentrated and intense infusion. To further explore this phenomenon, we conducted additional experiments using an

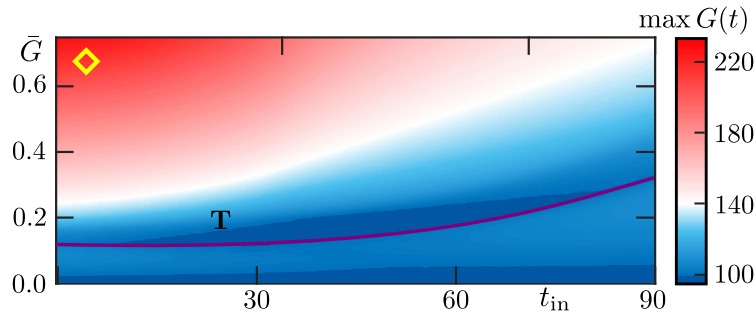


Figure 5. Response of model (1)–(2) to glucose infusion protocol (13) with average infusion rate $\bar{G} = G_{\max} \cdot t_{\text{in}}/T_{\text{in}}$ mg dl⁻¹ min⁻¹ over the length of infusion t_{in} (min) with constant period $T_{\text{in}} = 180$ (min). Shown is the maximum value of G (mg/dl) in colorcode (blue-white) obtained by integration for various t_{in} and \bar{G} . The maximum data is overlaid by curves of torus bifurcation (purple), curves of fold bifurcation of periodic orbits (red) and curves of period doubling bifurcation (purple) bounding regions of locking to the infusion protocol. Other parameters are $\tau_I = 5$ min and $\tau_G = 20$ min.

on-off glucose infusion protocol with a fixed infusion period of $T_{\text{in}} = 180$ min. Figure 5 showcases the results obtained from these experiments, where we varied both the infusion time t_{in} and the average glucose dose per minute \bar{G} , represented by $G_{\max} \cdot t_{\text{in}}/T_{\text{in}}$.

In this figure, we observe a locus in the parameter space that corresponds to the quasi-periodic orbit illustrated in Fig. 1(e). This locus is denoted by a distinctive yellow diamond marker, which highlights the specific combination of infusion time and glucose dose that leads to the observed quasi-periodic behavior. Additionally, we present a curve labeled as **T**, which represents a torus bifurcation curve. This curve serves as an indicator of the critical transition point between entrainment and quasi-periodic oscillation in response to the infusion protocol.

Discussion

It is well documented that glucose rhythms stimulate pulsatile pancreatic insulin secretion at various timescales^{29,34}. For example, the 1:1 entrainment mode – namely one ultradian glucose oscillation per glucose infusion cycle – was clinically shown to be present using a sinusoidal glucose infusion in individuals without diabetes^{8,19}. Our analysis of periodically driven ultradian oscillations highlights that a periodic on-off stimulus, closer to normal daily conditions, also possesses the ability to entrain glucose rhythms. Furthermore, the duration of each glucose input has a crucial impact on the generation of periodic rhythms, as well as on attained glycemic levels. This theoretically provides a method for delivering a fixed glucose dose while minimising the amplitude of the resulting rhythm. This can be achieved by either altering the period of the infusion, or the length of each pulse. This is most observable in figure 5, where stretching the infusion duration leads to lower glucose amplitudes. For example, consider a scenario where glucose is infused every 180 minute over a 12-hour period. Infusing a dose with $G_{\max} = 2.4$ mg dl⁻¹ min⁻¹ over $t_{\text{in}} = 30$ minutes leads to a maximal glucose value around 150 mg/dl. In contrast, a dose with $G_{\max} = 1.2$ mg dl⁻¹ min⁻¹ over $t_{\text{in}} = 60$ minutes reduces the maximal glucose level to around 125 mg/dl. In both cases, the average dose per minute is $\bar{G} = 0.4$ mg dl⁻¹ min⁻¹, and a total dose of 288 mg/dl is infused over the 12 hour timespan.

Our study provides valuable insights into the system's response to glucose infusion patterns, providing multiple pathways for the production of stable oscillatory rhythms and a similar entrainment structure is also expected for simpler models of glucose-insulin regulation featuring delays, e.g.^{30,35,36}. Nonetheless, there are several limitations that should be considered. First, let us note that while the exact location of bifurcation curves would depend on model parameters, the bifurcation types are likely to remain the same for parameter ranges representing non-diabetic individuals. Our model assumes fixed values for the delays in insulin and glucose production pathways, represented by τ_I and τ_G respectively. In reality, these delays can vary between individuals and change over short and long timescales due to daily-life factors such as exercise, aging and the presence of insulin resistance. Future research could incorporate individual-specific delays to account for this variability and investigate their impact on the system's dynamics.

It is worth noting that our model relies solely on plasma glucose and insulin measurements for prediction, which highlights the importance of accurate and reliable measurements in clinical settings. The nonlinear structure of the model allows for the description of nontrivial dynamics and enhances parameter identifiability. This aspect is crucial for developing robust and accurate models

that can capture the complex dynamics of the glucose-insulin regulatory system.

It is also worth noting that the timing of the glucose infusion does not influence the bifurcation structure (4), nor the glucose-insulin ranges of the periodic rhythms. In other words, the long term dynamics is not dependent on the starting time of the periodic on-off glucose infusion. This does not mean that the timing of glucose inputs bears little importance. While the investigated infusion ranges ensured the positivity of glucose and insulin values, values below or above healthy physiological ranges may appear in the transient path to the limit cycle. In turn, additional dynamics may emerge from interactions with other physiological feedback loops or subsystems, such as the glucagon pathway or the hypothalamic-pituitary-adrenal axis, for which the alignment with glucose regulation is essential for maintaining good health³⁷. The recent incorporation of glucagon²² in models of the glucose-insulin feedback system may help provide a more complete and quantitative picture of dynamical interactions occurring within the pancreas^{38,39} which can be used to improve quantitative tests for the detection and measurement of insulin and glucagon resistance⁴⁰.

Another aspect to consider is the interaction between the glucose-insulin regulatory system and other physiological processes. Our model focuses solely on the glucose-insulin loop, but in reality, there are complex interactions between various metabolic pathways, hormones, and organs. Integrating these interactions into a comprehensive model could provide a more complete understanding of the system's behavior and its response to different stimuli.

Conclusion

In this study, we employed a system-level mathematical model to investigate the response of the glucose-insulin regulatory system to periodic glucose infusion. By exploring different glucose infusion patterns and analyzing the resulting dynamics, we gained insights into the system's behavior and identified key factors influencing its response.

Our findings demonstrate that the glucose-insulin regulatory system exhibits a range of behaviors depending on the glucose infusion pattern. When a constant glucose infusion is applied, the system shows ultradian oscillations characterized by periodic variations in glucose and insulin levels. However, as the glucose infusion rate exceeds a certain threshold, these oscillations disappear, and the system focuses on reducing glucose levels without exhibiting oscillatory behavior. This observation suggests a physiological limit beyond which the system's oscillatory capacity is overwhelmed.

We further investigated the effects of periodic on-off pulses, mimicking repeated intravenous glucose tolerance tests. Our analysis revealed that the period of the on-off pulses plays a crucial role in determining the system's dynamics and glucose-insulin ranges. Different patterns of oscillations, including stable limit cycles and irregular oscillations, were observed for varying infusion periods. This highlights the importance of considering the frequency and duration of glucose stimuli in understanding the system's response.

The results of this study have important implications for understanding glucose regulation in both normal and abnormal physiological conditions. By elucidating the system's response to different glucose infusion patterns, our findings can inform the development of test strategies for evaluating the system's performance and identifying potential dysfunctions. Furthermore, they provide insights into the underlying mechanisms governing glucose-insulin dynamics, contributing to the broader understanding of metabolic regulation.

In conclusion, our study enhances our understanding of the glucose-insulin regulatory system by investigating its response to periodic glucose infusion. We identified the impact of different glucose infusion patterns on the system's dynamics and demonstrated the importance of various types of glucose stimuli. These insights can aid in the development of diagnostic and therapeutic strategies for glucose regulation and contribute to advancements in the management of metabolic disorders. Future research should aim to incorporate individual-specific delays and consider the broader physiological context to further refine our understanding of glucose regulation and its implications for human health.

Methods

The glucose-insulin regulatory delayed-feedback model

We consider the system-level mathematical model

$$G'(t) = G_{in}(t) - f_2(G(t)) - f_3(G(t))f_4(I(t)) + f_5(I(t - \tau_G)) \quad (1)$$

$$I'(t) = I_{in}(t) + f_1(G(t - \tau_I)) - dI(t) \quad (2)$$

with variables $I(t)$ and $G(t)$ representing the concentrations and of glucose (mg dl^{-1}) and insulin (uU ml^{-1}) in the plasma at time instant t . System (1)–(2) explicitly depends on time delays τ_I and

τ_G respectively representing the system's response time to insulin production as a result to glucose uptake, and the production of glucose by the liver as a result of low insulin levels. Glucose intake and insulin infusion are modeled by parameters, here called G_{in} and I_{in} . The physiological response of body is modeled by the nonlinearities

$$\begin{aligned} f_1(G) &= \frac{R_m G^{h_1}}{G^{h_1} + (V_g k_1)^{h_1}}, \\ f_2(G) &= \frac{U_b G^{h_2}}{G^{h_2} + (V_g k_2)^{h_2}}, \\ f_3(G) &= \frac{G}{C_3 V_g}, \\ f_4(I) &= U_0 + \frac{(U_m - U_0) I^{h_4}}{I^{h_4} + (1/V_i + 1/(E t_i))^{-h_4} k_4^{h_4}}, \\ f_5(I) &= \frac{R_g I^{h_5}}{I^{h_5} + (V_p k_5)^{h_5}}, \end{aligned}$$

where $R_m = 210$, $V_i = 11$, $V_g = 10$, $E = 0.2$, $U_b = 72$, $t_i = 100$, $C_3 = 1000$, $R_g = 180$, $U_0 = 40$, $V_p = 3$, $U_m = 940$, $h_1 = 2$, $k_1 = 6000$, $h_2 = 1.8$, $k_2 = 103.5$, $h_4 = 1.5$, $k_4 = 80$, $h_5 = -8.54$, and $k_5 = 26.7$ with corresponding units. Insulin degradation is modeled by a constant rate d . Throughout the paper we fix $d = 0.06$. The model has been considered before and has been analyzed extensively by various authors^{20,26–28}. In particular, it can be shown that, for the parameter values considered and in the absence of infusion, there is a unique equilibrium solution (G^*, I^*) ; see for example [41]. The delay parameters used for numerical simulation are $\tau_I = 5$ and $\tau_G = 20$ if not stated otherwise. For the general theory of delay differential equations, such as existence, uniqueness and the stability of solutions, we refer the interested reader to classic textbooks on the topic^{42,43}.

Critical delay values for oscillatory behavior when infusion rate is constant

The critical curve for oscillations in the (τ_I, τ_G) -parameter plane can be computed from the linearization of system (1)–(2) about the equilibrium solution (G^*, I^*) and imposing the condition $\lambda = i\omega$, $\omega > 0$ (Hopf bifurcation) on solutions of the corresponding characteristic equation

$$0 = \chi(\lambda) := \lambda^2 + \alpha_1 \lambda + \alpha_0 + \beta_1 e^{-\lambda \tau_1} + \beta_2 e^{-\lambda \tau_2}, \quad (3)$$

where $\tau_1 = \tau_I$, $\tau_2 = \tau_I + \tau_G$ and $\alpha_1 = f_2'(G^*) + f_3'(G^*)f_4(I^*) + d$, $\alpha_0 = d(f_2'(G^*) + f_3'(G^*)f_4(I^*))$, $\beta_1 = f_1'(G^*)f_3(G^*)f_4'(I^*)$, $\beta_2 = -f_1'(G^*)f_5'(I^*)$. A detailed derivation of Eq. (3) can be found in [28].

The equation $0 = \chi(i\omega)$ can be solved parametrically for τ_1 and τ_2 to give

$$\tau_{1,2}(\omega) = \frac{1}{\omega} \left(\arctan \left(\frac{\alpha_1 \omega}{\omega^2 - \alpha_0} \right) + \arccos \left(\frac{\beta_{2,1}^2 - \beta_{1,2}^2 - (\omega^2 - \alpha_0)^2 - \alpha_1^2 \omega^2}{2\beta_{1,2} \sqrt{(\omega^2 - \alpha_0)^2 + \alpha_1^2 \omega^2}} \right) \right), \quad (4)$$

revealing the critical curve for oscillations $\mathbf{H} \subset \mathbb{R}^2$ (curve of Hopf bifurcation)

$$\mathbf{H}(\omega) = (\tau_I(\omega), \tau_G(\omega)) = (\tau_1(\omega), \tau_2(\omega) - \tau_1(\omega)). \quad (5)$$

For the considered parameter values, we have that $\alpha_1 > \alpha_0$ and $\beta_2 > \alpha_0$, ensuring the existence of \mathbf{H} . Indeed the curve is a sharp threshold for oscillation, as it can be shown numerically that for positive values (τ_I, τ_G) below \mathbf{H} the fixed point (G^*, I^*) is stable for any physiological range of starting values G and I . It is worth noting here that system (1)–(2) undergoes further Hopf bifurcations, respectively at $\tau_{I,k}(\omega) = \tau_I(\omega) + 2\pi k/\omega$ and $\tau_{G,l}(\omega) = \tau_G(\omega) + 2\pi l/\omega$ with k, l an integer; however, for the parameter values considered, we can restrict ourselves to the smallest positive such value pair to cover the physiological parameter range. The range of relevant values of ω resulting in positive delays cannot be computed explicitly, however, straightforward calculations show that the boundaries ω_I, ω_G satisfying $\tau_I(\omega_I) = 0$ and $\tau_G(\omega_G) = 0$ are given by

$$\omega_G = \sqrt{\alpha_0 - \frac{\alpha_1^2}{2} + \sqrt{\left(\alpha_0 - \frac{\alpha_1^2}{2}\right)^2 + (\beta_1 + \beta_2)^2 - \alpha_0^2}}, \quad (6)$$

$$\omega_I = \sqrt{\alpha_0 + \beta_1 - \frac{\alpha_1^2}{2} + \sqrt{\left(\alpha_0 + \beta_1 - \frac{\alpha_1^2}{2}\right)^2 + \beta_2^2 - \alpha_0^2}}, \quad (7)$$

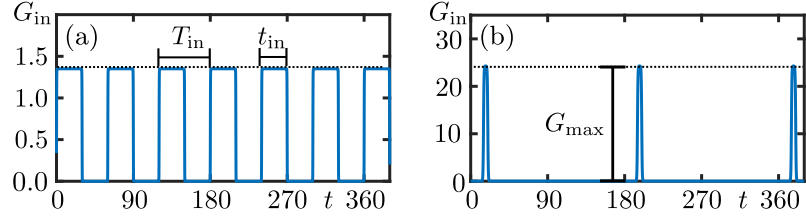


Figure 6. Form of glucose infusion used to obtain Figs. 1(d)–(e).

with the corresponding delay values

$$\tau_I(\omega_G) = \frac{1}{\omega_G} \arctan\left(\frac{\alpha_1 \omega_G}{\omega_G^2 - \alpha_0}\right) + \frac{2\pi k^*}{\omega_G}, \quad (8)$$

$$\tau_G(\omega_I) = \frac{1}{\omega_I} \arctan\left(\frac{\alpha_1 \omega_I}{\omega_I^2 - \alpha_0 - \beta_1}\right) + \frac{2\pi l^*}{\omega_I}, \quad (9)$$

where k^*, l^* are the smallest integers such that τ_G and τ_I are positive.

We remark that the curve \mathbf{H} vaguely resembles a straight line with slope -1 in the (τ_I, τ_G) -plane. This can be understood by exploiting the fact that parameter β_1 is small on the order of 10^{-3} . Imposing the regular perturbation ansatz $\omega = \omega_0 + \beta_1 \omega_1 + \mathcal{O}(\beta_1^2)$ on the imaginary part of (3) and comparing at zeroth and first order in β_1 , we formally obtain

$$\omega_0 = \sqrt{\alpha_0 - \frac{\alpha_1^2}{2}} + \sqrt{\left(\alpha_0 - \frac{\alpha_1^2}{2}\right)^2 + \beta_2^2 - \alpha_0^2}, \quad (10)$$

$$\omega_1 = \frac{\omega_0}{\alpha_1 - \alpha_0 + \omega_0^2} \tau_I \leq \frac{1}{2\sqrt{\alpha_1 - \alpha_0}} \tau_I. \quad (11)$$

Thus, we can approximate \mathbf{H} to first order in β_1

$$\mathbf{H}(\omega_0 + \beta_1 \omega_1(\tau_I)) \approx (\tau_I, \tau_2(\omega_0 + \beta_1 \omega_1(\tau_I)) - \tau_I) \quad (12)$$

by using the expression $\tau_2(\omega)$ in (4). As a result, \mathbf{H} approaches the graph of the function $\tau_I \mapsto \tau_2(\omega_0) - \tau_I$ with slope -1 as $\beta_1 \rightarrow 0$, which can be considered as a zero order approximation of \mathbf{H} .

On-off periodic infusion

Periodic shot infusion is modeled by a smooth, periodic, quickly varying function between $G_{in}(t) = I_{in}(t) = 0$ in mg/(dl·min) (no infusion) and $G_{in}(t) = G_{max}$ (glucose infusion), respectively. We consider the specific form

$$G_{in}(t) = G_{max} \cdot s(t - \sigma_G), \quad s(t) = h(\sin(2\pi t/T_{in})) \cdot h(\sin(2\pi(t - t_{in})/T_{in} - \pi)), \quad (13)$$

where the sigmoidal function $h(y) = (1 + \exp(-ky))^{-1}$ can be considered a smooth version of the Heaviside step function $H(y) = 0$ if $y < 0$, and $H(y) = 1$ if $y \geq 0$ for sufficiently large k . The form of (13) was inspired by a model for auditory perception⁴⁴. T_{in} is the time between consecutive shots of glucose/insulin with duration t_{in} , and the lag σ_G can be used to specify the timing of the infusion with respect to the underlying oscillation. The parameter k models the initial and terminal variations at the beginning and end of the shot application. A detailed analysis of the influence of the k -parameter is beyond the scope of this paper. We found the choice $k = 100$ to be sufficient. Panels (a) and (b) of Figure 6 show the shape of the infusion patterns used for numerical computation of time series in Fig. 1.

Numerical bifurcation analysis of time-delay systems with periodic infusion

Numerical simulations have been obtained using pydelay⁴⁵. Numerical bifurcation analysis has been performed using the software package DDE-BIFTOOL for Matlab/Octave³³. For a general introduction to numerical continuation methods available for delay differential equations and their application to physiological systems see Refs. 46 and³², respectively. Isocurves in Fig. 2 have been computed using numerical continuation of periodic orbits in two parameters with the additional condition fixed period (a), and fixed maximum value (b), fixed maximum value (c), where in cases

(b) and (c) we also relaxed the phase condition. For bifurcation analysis in the presence of periodic infusion, we append the two-dimensional ordinary differential equation

$$x'(t) = x - \omega y(t) - x(t)(x(t)^2 + y(t)^2), \quad (14)$$

$$y'(t) = -\omega x(t) + y - y(t)(x(t)^2 + y(t)^2), \quad (15)$$

with known stable periodic solution $(x(t), y(t)) = (\cos(\omega t), \sin(\omega t))$ to system (1)–(2). The method has been employed in several other works, see for example Ref. 47. We achieve the specific form of infusion (13) by setting $G_{in}(t) = G_{max}h(y(t - \sigma_G))h(y(t - \sigma_G - t_{in}\omega - \pi))$, where $\omega = 2\pi/T_{in}$.

References

1. Goldbeter, A. & Yan, J. Multi-synchronization and other patterns of multi-rhythmicity in oscillatory biological systems. *Interface Focus*. **12**, 20210089 (2022).
2. Keener, J. & Sneyd, J. *Mathematical physiology: II: Systems physiology* (Springer, 2009).
3. Sweeney, E. L., Jeromson, S., Hamilton, D. L., Brooks, N. E. & Walshe, I. H. Skeletal muscle insulin signaling and whole-body glucose metabolism following acute sleep restriction in healthy males. *Physiol. reports* **5**, e13498 (2017).
4. Sweeney, E. L., Peart, D. J., Ellis, J. G. & Walshe, I. H. Impairments in glycaemic control do not increase linearly with repeated nights of sleep restriction in healthy adults: a randomised controlled trial. *Appl. Physiol. Nutr. Metab.* **46**, 1091–1096 (2021).
5. Spiga, F., Walker, J. J., Terry, J. R. & Lightman, S. L. Hpa axis-rhythms. *Compr. physiology* **4**, 1273–1298 (2011).
6. Grant, A. D., Wilsterman, K., Smarr, B. L. & Kriegsfeld, L. J. Evidence for a coupled oscillator model of endocrine ultradian rhythms. *J. biological rhythms* **33**, 475–496 (2018).
7. Scheen, A. J., Byrne, M. M., Plat, L., Leproult, R. & Van Cauter, E. Relationships between sleep quality and glucose regulation in normal humans. *Am. J. Physiol. And Metab.* **271**, E261–E270 (1996).
8. O’Meara, N. M., Sturis, J., Van Cauter, E., Polonsky, K. S. *et al.* Lack of control by glucose of ultradian insulin secretory oscillations in impaired glucose tolerance and in non-insulin-dependent diabetes mellitus. *The J. clinical investigation* **92**, 262–271 (1993).
9. Committee, A. D. A. P. P. 6. Glycemic Targets: Standards of Medical Care in Diabetes—2022. *Diabetes Care* **45**, S83–S96, DOI: [10.2337/dc22-S006](https://doi.org/10.2337/dc22-S006) (2021). https://diabetesjournals.org/care/article-pdf/45/Supplement_1/S83/637560/dc22s006.pdf.
10. Ajmera, I., Swat, M., Laibe, C., Le Novere, N. & Chelliah, V. The impact of mathematical modeling on the understanding of diabetes and related complications. *CPT: pharmacometrics & systems pharmacology* **2**, 1–14 (2013).
11. Makroglou, A., Li, J. & Kuang, Y. Mathematical models and software tools for the glucose-insulin regulatory system and diabetes: an overview. *Appl. numerical mathematics* **56**, 559–573 (2006).
12. Palumbo, P., Ditlevsen, S., Bertuzzi, A. & De Gaetano, A. Mathematical modeling of the glucose–insulin system: A review. *Math. biosciences* **244**, 69–81 (2013).
13. Huard, B. & Kirkham, G. Mathematical modelling of glucose dynamics. *Curr. Opin. Endocr. Metab. Res.* 100379 (2022).
14. Bergman, R. N., Ider, Y. Z., Bowden, C. R. & Cobelli, C. Quantitative estimation of insulin sensitivity. *Am. J. Physiol. And Metab.* **236**, E667 (1979).
15. Bergman, R. N. Origins and history of the minimal model of glucose regulation. *Front. Endocrinol.* **11**, 583016 (2021).
16. Ha, J., Muniyappa, R., Sherman, A. S. & Quon, M. J. When minmod artifactually interprets strong insulin secretion as weak insulin action. *Front. physiology* 508 (2021).
17. Walker, J. J., Terry, J. R. & Lightman, S. L. Origin of ultradian pulsatility in the hypothalamic–pituitary–adrenal axis. *Proc. Royal Soc. B: Biol. Sci.* **277**, 1627–1633 (2010).
18. Zavala, E. *et al.* Mathematical modelling of endocrine systems. *Trends Endocrinol. & Metab.* **30**, 244–257 (2019).
19. Sturis, J. *et al.* Phase-locking regions in a forced model of slow insulin and glucose oscillations. *Chaos: An Interdiscip. J. Nonlinear Sci.* **5**, 193–199 (1995).

20. Li, J., Kuang, Y. & Mason, C. C. Modeling the glucose–insulin regulatory system and ultradian insulin secretory oscillations with two explicit time delays. *J. theoretical biology* **242**, 722–735 (2006).
21. Chen, C.-L., Tsai, H.-W. & Wong, S.-S. Modeling the physiological glucose–insulin dynamic system on diabetics. *J. theoretical biology* **265**, 314–322 (2010).
22. Cohen, R. B. & Li, J. A novel model and its analysis on the metabolic regulations of glucose, insulin, and glucagon. *SIAM J. on Appl. Math.* **81**, 2684–2703 (2021).
23. Glass, D. S., Jin, X. & Riedel-Kruse, I. H. Nonlinear delay differential equations and their application to modeling biological network motifs. *Nat. communications* **12**, 1788 (2021).
24. McKenna, J. P., Dhumpa, R., Mukhitov, N., Roper, M. G. & Bertram, R. Glucose oscillations can activate an endogenous oscillator in pancreatic islets. *PLoS computational biology* **12**, e1005143 (2016).
25. Bruce, N. *et al.* Coordination of pancreatic islet rhythmic activity by delayed negative feedback. *Am. J. Physiol. Metab.* **323**, E492–E502, DOI: [10.1152/ajpendo.00123.2022](https://doi.org/10.1152/ajpendo.00123.2022) (2022).
26. Li, J. & Kuang, Y. Analysis of a model of the glucose–insulin regulatory system with two delays. *SIAM J. on Appl. Math.* **67**, 757–776 (2007).
27. Huard, B., Easton, J. F. & Angelova, M. Investigation of stability in a two-delay model of the ultradian oscillations in glucose–insulin regulation. *Commun. Nonlinear Sci. Numer. Simul.* **26**, 211–222 (2015).
28. Huard, B., Bridgewater, A. & Angelova, M. Mathematical investigation of diabetically impaired ultradian oscillations in the glucose–insulin regulation. *J. theoretical biology* **418**, 66–76 (2017).
29. Sturis, J., Polonsky, K., Mosekilde, E. & Van Cauter, E. Computer model for mechanisms underlying ultradian oscillations of insulin and glucose. *Am J Physiol* **260**, E801–E809 (1991).
30. Shi, X., Kuang, Y., Makroglou, A., Mokshagundam, S. & Li, J. Oscillatory dynamics of an intravenous glucose tolerance test model with delay interval. *Chaos: An Interdiscip. J. Nonlinear Sci.* **27**, 114324 (2017).
31. Kuznetsov, Y. A. *Elements of applied bifurcation theory*, vol. 112 (Springer, 1998).
32. Engelborghs, K., Luzyanina, T. & Roose, D. Numerical bifurcation analysis of delay differential equations using dde-biftool. *ACM Transactions on Math. Softw. (TOMS)* **28**, 1–21 (2002).
33. Sieber, J., Engelborghs, K., Luzyanina, T., Samaey, G. & Roose, D. Dde-biftool v. 3.0 manual—bifurcation analysis of delay differential equations. *arXiv preprint arXiv:1406.7144* (2014).
34. Satin, L. S., Butler, P. C., Ha, J. & Sherman, A. S. Pulsatile insulin secretion, impaired glucose tolerance and type 2 diabetes. *Mol. aspects medicine* **42**, 61–77 (2015).
35. Panunzi, S., Palumbo, P. & De Gaetano, A. A discrete single delay model for the intra-venous glucose tolerance test. *Theor. Biol. Med. Model.* **4**, 35, DOI: [10.1186/1742-4682-4-35](https://doi.org/10.1186/1742-4682-4-35) (2007).
36. Li, J., Wang, M., Gaetano, A. D., Palumbo, P. & Panunzi, S. The range of time delay and the global stability of the equilibrium for an IVGTT model. *Math. Biosci.* **235**, 128–137, DOI: [10.1016/j.mbs.2011.11.005](https://doi.org/10.1016/j.mbs.2011.11.005) (2012).
37. Zavala, E. Misaligned hormonal rhythmicity: Mechanisms of origin and their clinical significance. *J. Neuroendocrinol.* **34**, e13144 (2022).
38. Pedersen, M. G., Mosekilde, E., Polonsky, K. S. & Luciani, D. S. Complex patterns of metabolic and ca^{2+} entrainment in pancreatic islets by oscillatory glucose. *Biophys. J.* **105**, 29–39, DOI: <https://doi.org/10.1016/j.bpj.2013.05.036> (2013).
39. Montefusco, F., Cortese, G. & Pedersen, M. G. Heterogeneous α -cell population modeling of glucose-induced inhibition of electrical activity. *J. theoretical biology* **485**, 110036 (2020).
40. Morettini, M. *et al.* Mathematical model of glucagon kinetics for the assessment of insulin-mediated glucagon inhibition during an oral glucose tolerance test. *Front. endocrinology* **12**, 611147 (2021).
41. Bennett, D. & Gourley, S. Global stability in a model of the glucose–insulin interaction with time delay. *Eur. J. Appl. Math.* **15**, 203–221 (2004).
42. Hale, J. K. & Lunel, S. M. V. *Introduction to functional differential equations*, vol. 99 (Springer Science & Business Media, 2013).

43. Diekmann, O., Van Gils, S. A., Lunel, S. M. & Walther, H.-O. *Delay equations: functional-, complex-, and nonlinear analysis*, vol. 110 (Springer Science & Business Media, 2012).
44. Ferrario, A. & Rankin, J. Auditory streaming emerges from fast excitation and slow delayed inhibition. *The J. Math. Neurosci.* **11**, 1–32 (2021).
45. Flunkert, V. & Schoell, E. Pydelay-a python tool for solving delay differential equations. *arXiv preprint arXiv:0911.1633* (2009).
46. Krauskopf, B. & Sieber, J. Bifurcation analysis of systems with delays: Methods and their use in applications. In *Controlling delayed dynamics: advances in theory, methods and applications*, 195–245 (Springer, 2022).
47. Keane, A., Krauskopf, B. & Postlethwaite, C. Delayed feedback versus seasonal forcing: Resonance phenomena in an el niño southern oscillation model. *SIAM J. on Appl. Dyn. Syst.* **14**, 1229–1257 (2015).

Acknowledgements (not compulsory)

The authors thank Jan Sieber for helpful discussions on the implementation of the numerical continuation methods in DDE-BIFTOOL.

Author contributions statement

S.R. and B.H contributed equally to the study. Both authors conducted numerical experiments, analyzed the results, and contributed to the draft of the manuscript. Both authors reviewed the manuscript.

Data available statement

Numerical procedures to generate figures are available from the corresponding author on reasonable request.

Additional information

The authors declare no competing interests.